ARTICLE OPEN



Intact corticostriatal function in aged system x_c - deficient mice

Laura De Pauw¹, Agnès Villers (1)², Cindy Moore³, Olaya Lara (1)¹, Océane Vanonckelen¹, Lise Verbruggen¹, Hideyo Sato⁴, Eduard Bentea¹, Lutgarde Arckens (1)⁵, Laurence Ris (1)², Gamze Ates (1)¹, Charles K. Meshul³ and Ann Massie (1)¹

© The Author(s) 2025

System x_C⁻ (with xCT as specific subunit) is an astrocytic cystine/glutamate antiporter that constitutes the major source of extracellular glutamate in the mouse striatum. We previously reported that young-adult mice lacking xCT (xCT^{-/-} mice) display decreased intracellular glutamate levels in pre- and post-synaptic compartments at corticostriatal synapses as well as impaired corticostriatal neurotransmission, compared to wildtype (xCT^{+/+}) littermates. These changes were accompanied by increased repetitive behavior and reduced social interaction, typical behaviors related to autism spectrum disorder (ASD). Although ASD is reported to be associated with atypical brain aging, we recently showed that xCT^{-/-} mice are protected against age-related hippocampal decline. Therefore, we here investigated whether the corticostriatal impairments and associated ASD-like behavior would be maintained in aged (16-months-old) mice. Genetic deletion of xCT does not affect corticostriatal neurotransmission in aged mice or the morphology of medium-spiny neurons. Except for a slight decrease in synaptic cleft width, the ultrastructure of corticostriatal synapses and intracellular glutamate levels are unaltered in the absence of xCT in aged mice. Accordingly, repetitive and social explorative behavior were comparable between aged xCT^{-/-} mice, while the latter showed a reduction in interactions that could be classified as being aggressive or dominant. To conclude, contrary to our previous observations in young-adult mice, corticostriatal neurotransmission and social behavior are no longer impaired in aged xCT^{-/-} mice, most likely because intracellular glutamate levels are no longer different. Moreover, the reduced levels of advanced glycation end-products that we observed in striatal tissue of xCT^{-/-} mice, can protect the xCT^{-/-} brain from age-related pathogenic alterations.

Translational Psychiatry (2025)15:471; https://doi.org/10.1038/s41398-025-03686-9

INTRODUCTION

System x_c^- is a cystine/glutamate antiporter that imports cystine in exchange for glutamate. It consists of the specific subunit xCT (SLC7A11) that regulates the transport function of the antiporter, and a 4F2 heavy chain that anchors xCT in the membrane [1]. System x_c is mainly expressed on the glial cells of the central nervous system (CNS) and cells of the innate immune system, and its expression is enhanced by e.g. inflammatory stimuli and oxidative stress [1]. Although the imported cystine will be reduced into cysteine that can be used to produce glutathione (GSH) -one of the most important antioxidants of the body- until now there is no in vivo evidence for increased oxidative stress or reduced antioxidant capacity in the CNS of system x_c -deficient mice [2–4]. On the other hand, we previously reported that the exported glutamate accounts for 60-70% of the extracellular glutamate levels in striatum and hippocampus [2, 3]. Given this glutamate is considered to be released into the extrasynaptic space, it cannot only increase the excitotoxic threshold but also modulate glutamatergic neurotransmission by acting on extrasynaptic ionotropic and metabotropic glutamate receptors, respectively [4–9]. Accordingly, we showed that the absence of xCT protects mice in several models for neurological disorders [2, 10-12] and affects glutamate-sensitive behaviors, such as spatial working memory [4], anxiety-(13) and depressive-like behavior [13, 14]. In humans, xCT levels are increased in post-mortem tissue of patients with epilepsy [15], Alzheimer's disease [16], amyotrophic lateral sclerosis [17] and multiple sclerosis [18, 19], compared to (agematched) healthy controls. In patients with malignant glioma, tumor xCT expression is associated with seizures and predicts poor survival [20].

In young-adult mice, however, genetic xCT deletion (xCT^{-/-} mice) results in corticostriatal deficits. While no differences in the morphology of striatal medium spiny neurons (MSN) could be detected, decreased glutamate levels in pre- and post-synaptic compartments were present as well as impaired corticostriatal neurotransmission that could be rescued by glutamate supplementation [8]. Psychiatric disorders such as autism spectrum disorder (ASD) and obsessive-compulsive disorder (OCD) are linked to corticostriatal deficits [21-23] and glutamatergic dysregulation has been shown to contribute to the typical increased repetitive behavioral phenotype that is observed in mouse models for these disorders [24]. Accordingly, xCT^{-/-} mice showed increased repetitive behavior and social impairments that reflect ASD-like behavioral changes, compared to xCT^{+/+} mice [13]. In a recent study, the analysis of two distinct human gene expression data sets identified a causal relationship between

¹Neuro-Aging & Viro-Immunotherapy, Center for Neurosciences, Vrije Universiteit Brussel (VUB), Brussels, Belgium. ²Department of Neurosciences, Research Institute for Health Science and Technologies, Université de Mons (UMONS), Mons, Belgium. ³Department of Behavioral Neuroscience, Oregon Health & Science University and the Veterans Hospital Medical Center, Portland, OR 97239, USA. ⁴Department of Medical Technology, Niigata University, Niigata, Japan. ⁵Laboratory of Neuroplasticity and Neuroproteomics, and Leuven Brain Institute (LBI), Katholieke Universiteit Leuven (KU Leuven), Leuven, Belgium. [⊠]email: ann.massie@vub.be

Received: 28 April 2025 Revised: 8 September 2025 Accepted: 2 October 2025

Published online: 17 November 2025

disulfidptosis and ASD, and silencing xCT via stereotactic injection of anti-Slc7a11 siRNA virus into the mouse cortex improved ASD-like behavior in the BTBR mouse model for ASD [25].

While research on the aging process of the ASD brain is limited, it has been suggested that individuals with ASD show signs of atypical brain aging [26], with higher rates of cognitive disorders reported in older people with ASD [27]. We, however, recently reported that the deletion of xCT results in protection against agedecline in hippocampal neurotransmission hippocampus-dependent spatial memory. These protective effects were accompanied by changes in the hippocampal metabolome, with the most important metabolite to separate aged xCT^{+/+} and xCT^{-/-} mice being an advanced glycation end product (AGE) [4]. AGEs are formed by the non-enzymatic glycation of proteins, lipids and nucleic acids. They are known to accumulate with age, and besides their intrinsic capacity to damage (sub)cellular structures, the binding of AGEs to the AGE receptor RAGE evokes an inflammatory response potentially causing further harm to the surrounding tissue (for review, [28]). Patients with ASD are reported to have increased plasma and brain protein AGEs [29, 30].

In the current study, we therefore investigated corticostriatal neurotransmission, MSN morphology and ultrastructural properties of the corticostriatal synapses, as well as repetitive behavior and social interaction in aged mice with a genetic deletion of xCT. We show that system x_c- deficiency has no effect on corticostriatal function or social interaction in aged mice. While reduced extracellular glutamate levels and attenuated age-related (neuro-)inflammation can certainly benefit the aging process of the xCT^{/-} corticostriatal circuit, the reduced striatal AGE levels that we here observe could further explain our findings.

MATERIALS & METHODS

Mice

Male aged (16-months-old) $xCT^{+/+}$ (n = 22) and $xCT^{-/-}$ (n = 23) mice are high-generation descendants of the strain described previously [31] and were bred in a heterozygous colony in the animal facility of the Vrije Universiteit Brussel. Mice were grouphoused under standardized conditions (10/14 h dark/light cycle, 20–24 °C), with unlimited access to food and water.

Genotypes of the mice were confirmed by PCR on ear punch DNA using the REDExtract-N'Amp Tissue PCR Kit (Sigma-Aldrich), and the following primers: 5'-GATGCCCTTCAGCTCGATGCGGTTCACCAG-3' (GFPR3); 5'-CAGAGCAGCCCT AAGGCACTTTCC-3' (mxCT5flankF6); and 5'-CCGATGACGCTGCCGATGATGATGG-3' [mxCT(Dr4)R8].

Studies were performed according to national guidelines on animal experimentation and approved by the Ethical Committee for Animal Experimentation of the Vrije Universiteit Brussel.

All analyses were performed by a researcher blinded for genotype of the mice, and all recordings and images were analyzed in a random manner.

Slice electrophysiology

Slice electrophysiology was performed as described previously [8, 32]. Dissected brains were placed in a 4 °C artificial cerebrospinal fluid (aCSF) solution (124 mM NaCl, 4.4 mM KCl, 26 mM NaHCO₃, 1 mM NaH₂PO₄, 2.5 mM CaCl₂, 1.3 mM MgSO₄, 10 mM D-glucose) and oxygenated with a mixture of 95% O₂ and 5% CO₂. Brains were blocked and cut at a 30° angle using a vibratome. Slices with a thickness of 400 μ m were collected in aCSF. Undamaged slices were selected and transferred to a recording chamber where they could recover for 1.5 h at 28 °C under constant perfusion with oxygenated aCSF (1 ml/min). To stimulate the corticostriatal connections, a bipolar twisted nickel-chrome stimulating electrode (50 μ m diameter) was placed at the border of the corpus callosum, in close proximity to the recording glass microelectrode (filled with aCSF; resistance 2-5M Ω) that was

located in the dorsolateral region of the striatum. Cortical afferents were stimulated using biphasic constant-voltage pulses (0.08 ms for each pulse) at varying stimulus intensities between 5-15 V, inducing extracellular field excitatory postsynaptic potentials (fEPSPs) and generating a baseline input/output (I/O) curve. Paired-pulse response ratios were obtained by delivering two stimuli with an intensity that induces 50% of the maximal response, at various intervals (25, 50, 100, 200 and 400 ms).

Golgi-Cox staining

Golgi-Cox staining was performed as previously described [8]. Brains were stained using the FD Rapid GolgiStain kit (FD Neurotechnologies Inc.) and sliced into 80 µm vibratome sections [33]. For each mouse, 5-6 MSNs were imaged in the dorsolateral striatum using a bright field microscope (Zeiss Axio Imager Z.1) connected to an AxioCam MRc5 camera, using Zen2 (Blue edition, version 2.0.0.0; Carl Zeiss Microscopy GmBH). MSNs were included for analysis when the entire neuron was stained and the soma was round or ovoid [34]. Photomicrographs were taken at a 100x magnification and Z-stacks (0.5 µm/stack) were used to image the entire neuron throughout the thickness of the section. Neurons were manually traced on flattened Z-stack images using the software Neuromantic (V1.6.3) and their morphology (soma area, soma diameter, total dendritic length, number of primary dendrites and length of the longest dendrite) was evaluated using ImageJ (NIH), by an experimenter blinded to genotype. The mean of all neurons was calculated for each animal and considered as n = 1. Complexity of the dendritic tree was analyzed by Sholl analysis, where the number of intersections of the dendritic tree with concentric circles, placed around the cell body at increasing diameters in steps of 10 µm, was counted. Spine density was evaluated on dendritic segments of 12-28 µm in length.

Electron microscopy

Electron microscopy (EM) was performed and images of corticostriatal synapses were analyzed as previously described [8]. Slices containing the rostral dorsolateral striatum (1.0 mm anterior to Bregma) were processed for VGLUT1 pre-embedding 3,3'-diaminobenzidine (DAB) immunolabeling using a rabbit VGLUT1 antibody (1:1000, Synaptic Systems, cat. #135303) and a microwave procedure (Pelco BioWave, Ted Pella) as previously reported [35]. Next, the tissue slice was flat-embedded in epoxy, the dorsolateral striatum manually dissected and sectioned in thin slices of 60 nm. Slices were labelled with glutamate immunogold using a rabbit anti-glutamate antibody (1:250, Sigma-Aldrich, cat. #G6642) and a goat anti-rabbit IgG tagged with 18 nm gold particles (1:20, Jackson ImmunoResearch, cat. #111-215-144). Photomicrographs were taken of labelled terminals at a 40000x magnification, using a digital camera (AMT, Danvers, MA, USA). Terminals were selected for analysis if DAB-labelled synaptic vesicles were present and an asymmetrical synaptic contact with a dendritic spine or shaft could be detected. The number of immunogold particles located inside the nerve terminal and the mitochondria were counted. The glutamate density inside the presynaptic terminals was determined by subtracting the mitochondrial pool from the total nerve terminal pool. Several ultrastructural parameters (area and diameter of presynaptic terminal and spine heads, mitochondrial area, width of the synaptic cleft and area, thickness and length of the postsynaptic density (PSD)) were quantified using ImageJ software, in a random manner by an experimenter blind to the experimental conditions, as described previously [8]. For all parameters, the mean was calculated for each mouse, and this was considered n = 1.

Western blotting

Striatal tissue of aged $xCT^{+/+}$ and $xCT^{-/-}$ mice was homogenized in 300 μ l extraction buffer (2% SDS, 60 mM Tris base, 100 mM DTT, 1% phosphatase inhibitor cocktail 3, 1% protease inhibitor, pH

7.5). Equal concentrations of protein (12 µg) were loaded onto a 4-12% Bis-Tris gel (Bio-Rad Laboratories), separated under reducing conditions (SDS-PAGE) and transferred to a PVDF membrane. Nonspecific binding was blocked with a solution of 5% ECL membrane blocking agent (GE Healthcare) before overnight incubation at room temperature with goat anti-AGE (1:3000, Sigma-Aldrich, AB_11213078). The next day, membranes were incubated with rabbit anti-goat IgG secondary antibody (1:25000, Dako Agilent, AB_2617138) for 30 min. Immunoreactive bands were visualized using ECL prime (GE Healthcare) on an ImageQuant LAS 4000 detector. A total protein stain (ServaPurple, Serva Electrophoresis GmbH) was performed to allow normalization. Optical densities were measured using the Image Lab software (Bio-Rad Laboratories), normalized to the total protein stain and expressed relative to a pool sample. The Western blot was repeated twice.

Behavioral experiments

Behavioral analysis of the mice was performed between 9:00 am and 5:00 pm in an alternating manner between xCT^{+/+} and xCT^{-/-} mice. Behavioral tests were video-recorded using a webcam, and analyzed manually by an experimenter blinded for genotype.

We evaluated spontaneous social interaction using the reciprocal social interaction test. Two socially naive (i.e. non-littermate) genotype-matched mice were placed in a clean housing cage and allowed to interact with each other for 10 min. Time spent in noseto-nose sniffing, following, pushing past each other, crawling and mounting was analyzed. A sum of all parameters was made to get an indication of the total interaction time [36].

The three-chambered assay was performed in a box made of clear polycarbonate. The test consists of four phases. After 10 min of habituation to the centre chamber while the entrance to the two outer chambers is closed, the test mouse is allowed to explore the entire box, including both outer chambers (left-right bias; 10 min). Next, the mice were briefly confined to the centre chamber, while an inanimate object (inverted metal-wire cup) is placed in one of the side chambers, and a socially naive mouse is placed underneath an identical wire cup in the other side chamber (target mouse; weight-matched male 129/SvImJ mice that were trained for three consecutive days to remain calm underneath the metal-wire cup). The preference of the mouse to interact with the naive mouse is evaluated during a 10 min video-recorded trial (social preference test). Finally, after a short confinement in the centre chamber, the inanimate object is replaced by a novel mouse and the preference to interact with the novel mouse over the familiar mouse (socially naive mouse during previous phase), is evaluated (social novelty test). During both tests, the time spent interacting with the mouse, as well as the time spent and number of entries into each side chamber are quantified.

Repetitive behavior was evaluated with the marble burying test. Mice were individually placed in a regular housing cage with 5 cm of wood-chip bedding material. Fifteen black marbles were placed on top of this bedding material, in an equally spaced manner. Mice were videotaped for 15 min and analyzed for repetitive burying behavior. A marble was considered buried when more than two-thirds of its diameter was covered with bedding [37]. To avoid bias, motor function was evaluated on the acquired video files using Ethovision (Noldus).

Self-grooming behavior of the mice was analyzed for 30 min in an empty housing cage. Videos were analyzed for latency to grooming, number of grooming bouts and total time spent grooming. Analysis was performed as described previously [38].

Statistics

Data are presented as mean ± SEM. Statistical analyses were performed using GraphPad Prism 10 software. Normality of the data was checked using the D'Agostino-Pearson omnibus test and equality of variances with an F-test. For normally distributed data

with one variable and two groups to compare, an unpaired, two-tailed t-test was used. In case of unequal variances, the Welch's t-test was applied, whereas when data did not show a normal distribution, the non-parametric Mann-Whitney test was opted. When comparing the means of more than two groups, based on a single variable, a one-way ANOVA was used with a correction factor for multiple comparisons. To analyze the effect of two variables, a two-way ANOVA was performed and to interpret the results of the social novelty test, a repeated-measures two-way ANOVA was used. In case of significant main effects, the two-way ANOVA was followed by a Sidak's or Tukey's post-hoc test.

Some of the data presented in supplementary figures 4 and 5 did not show a normal distribution and were therefore log transformed before applying the parametric two-way ANOVA. However, for the ease of interpretation of the data, we show the graphs with the non-transformed data for all experiments. Outliers were identified using the Grubb's outlier test and excluded when significant (p < 0.05). Sample size estimation is based on our previous study in young mice [8]. All details regarding the statistical analyses are mentioned in figure legends.

RESULTS

Corticostriatal neurotransmission is similar in aged $xCT^{+/+}$ and $xCT^{/-}$ mice

The fEPSPs that were measured in the dorsolateral striatum after stimulating the corticostriatal fibers (Fig. 1A), were not different between aged xCT^{-/-} and xCT^{+/+} mice, resulting in overlapping I/O curves (Fig. 1B). Also, no differences in paired-pulse ratios can be detected for all investigated time intervals, indicating the absence of changes in short-term plasticity (Fig. 1C).

Decreased synaptic cleft width at corticostriatal synapses of aged xCT^{/-} mice, while the morphology of medium spiny neurons is unaltered

We could not observe any differences in the morphology of MSNs between aged xCT^{-/-} and xCT^{-/-} mice (Fig. 1D): soma area and diameter (Fig. 1E, F), number and length of dendrites (Fig. 1G–I), spine density (Fig. 1J, K) and the complexity of the dendritic tree (Fig. 1L) were unaltered.

Ultrastructural analysis of the corticostriatal synapses indicated the absence of differences in terminal (Fig. 2A, B), spine (Fig. 2C, D) and mitochondrial size (Fig. 2E) between aged xCT^{+/+} and xCT^{-/-} mice. Synaptic cleft width is smaller in aged xCT^{-/-} mice, compared to xCT^{+/+} mice (Fig. 2F), while PSD area (Fig. 2G), thickness (Fig. 2H) and length (Fig. 2I) were unaffected by xCT genotype. No changes were seen in glutamate levels in pre- and postsynaptic compartments or in mitochondria (Fig. 2J–L).

xCT deletion reduces striatal levels of advanced glycation endproducts

According to previous observations in hippocampal samples [4], striatal AGE protein levels are decreased in aged xCT^{-/-} compared to aged xCT^{+/+} mice (Fig. 3A, B).

xCT deletion does not influence repetitive behavior or social interest in aged mice, while aggressive behavior is attenuated In the marble burying test, aged xCT^{-/-} mice buried the same number of marbles (Fig. 4A, E) and spent an equal amount of time digging (Fig. 4B), compared to aged xCT^{+/+} mice. Also, the number of digging bouts (Fig. 4C) and the latency to start digging (Fig. 4D) were not affected by genotype. Finally, self-grooming behavior was comparable between aged xCT^{+/+} and xCT^{-/-} mice, reflected by similar total grooming time (Fig. 4F), number of grooming bouts (Fig. 4G) and latency to start grooming (Fig. 4H).

The genotype of the mice did not affect nose-to-nose sniffing (Fig. 5A), following (Fig. 5B) and pushing past each other in the reciprocal interaction test (Fig. 5C). Yet, aged xCT^{-/-} mice spent less

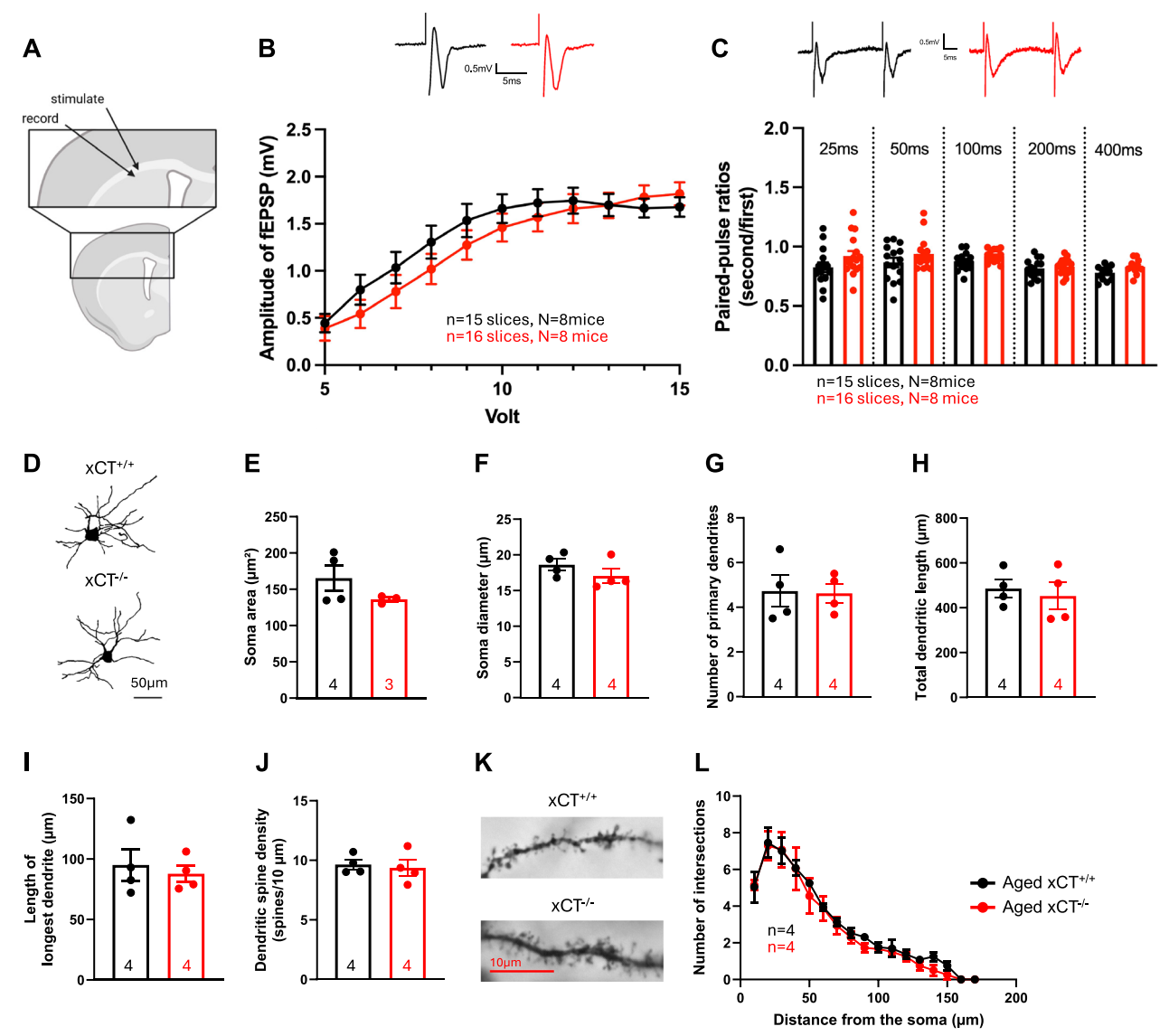
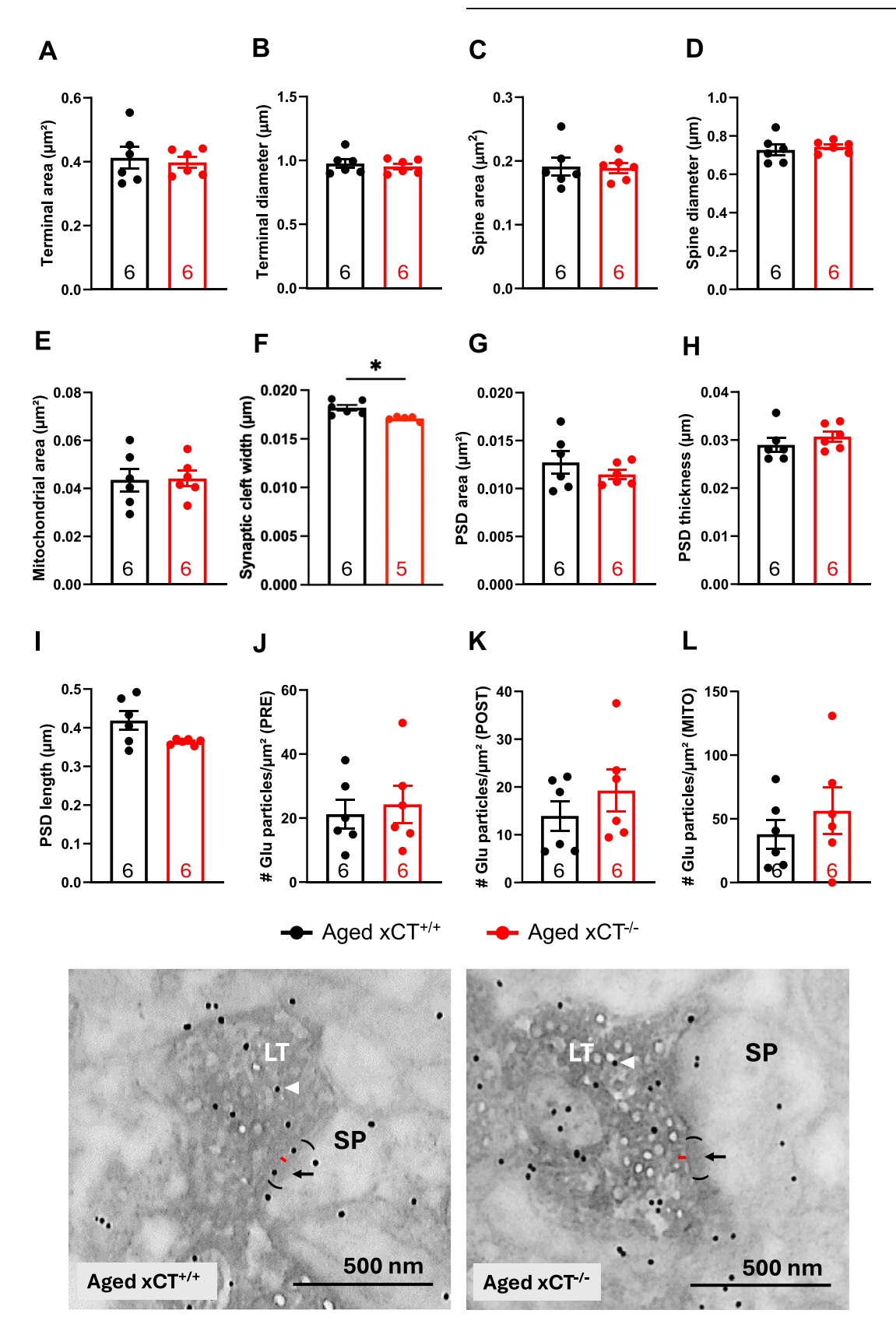


Fig. 1 Corticostriatal neurotransmission and morphological analysis of medium spiny neurons (MSN) in aged xCT^{+/+} and xCT^{-/-} mice. A Schematic representation (AP 0-0.5 mm relative to Bregma) of a striatal slice and positioning of stimulating and recording electrode (figure created with Biorender.com). B Input/Output (I/O) curves generated by stimulating corticostriatal fibers are similar between aged xCT^{+/+} and xCT^{-/-} mice. Inserts show a representative example of trace fEPSPs obtained at 12 V. C Paired-pulse ratios were similar between aged xCT^{+/+} and xCT^{-/-} mice, for all investigated time intervals. Inserts show a representative example of trace fEPSPs obtained at 6 V with an interval of 25 ms. Data are presented as mean \pm standard error of the mean (SEM) and analyzed using a two-tailed Mann-Whitney test for each stimulation intensity (B) or a one-way ANOVA with correction for repeated testing (C, at 100 ms one xCT^{-/-} outlier was excluded). A total number of 15 slices of n = 8 xCT^{+/+} mice (one slice was excluded due to technical issues) and 16 slices of n = 8 xCT^{-/-} mice were analyzed. D Representative tracing of medium spiny neurons (MSNs) of xCT^{+/+} and xCT^{-/-} mice. E-J No differences in soma area (E, one xCT^{-/-} outlier excluded) or diameter (F), number of primary dendrites (G), total dendritic length (H), length of longest dendrite (I) or dendritic spine density (J) between MSNs of aged xCT^{+/+} and xCT^{-/-} mice. K Representative picture of dendritic spines for both genotypes. L Using Scholl analysis, no effect on complexity of the dendritic tree was observed in the absence of xCT. 5-6 neurons of n = 4 xCT^{+/+} and n = 4 xCT^{-/-} mice were traced, with a total of 22 and 23 neurons respectively. Data are presented as mean \pm SEM and analyzed using an unpaired Welch's t-test (E) or a two-tailed unpaired t-test (F-L; at every distance from the soma for L).

time crawling (Fig. 5D) and mounting (Fig. 5E), compared to $xCT^{+/+}$ mice, behaviors that are considered being a sign of aggression and/ or dominance [39, 40]. Altogether, this results in equal social interest (Fig. 5G) and reduced aggressive/dominant behavior (Fig. 5H) in aged $xCT^{-/-}$ mice compared to their controls, while overall interaction time is decreased in the absence of xCT (Fig. 5F). Differences in aggressive behavior could not be linked to altered plasma testosterone levels between aged $xCT^{-+/+}$ and $xCT^{-/-}$ mice (Suppl. Figure 1).

During the social preference test of the three-chambered assay both aged xCT^{+/+} and xCT^{-/-} mice had an increased interest to

interact with the mouse, compared to the object. The time spent interacting with the mouse, did not differ between both genotypes (Fig. 5I), indicating that social interest was not affected by xCT deletion. Also, the time spent (Fig. 5J) or entries (Fig. 5K) in each chamber did not differ between both genotypes. Next, during the social novelty test, both aged xCT^{+/+} and xCT^{-/-} mice interacted more with the novel mouse compared to the familiar mouse (Fig. 5L), an effect that is most pronounced in the xCT^{-/-} mice, while the time spent and number of arm entries in each chamber was unaffected by genotype (Fig. 5M, N).



Aging levels down most behavioral differences between xCT $^{+/+}$ and xCT $^{\prime -}$ mice

We combined our current data with those we previously obtained in adult mice [8] and performed a two-way ANOVA, with aging and genotype as variables (Table 1, figures in supplement), to further obtain insight into why aged xCT^{/-} mice do not show the same impairments as the young-adult mice. While not all analyses could be compared due to elaborate inter-experiment time intervals (slice

Fig. 2 Ultrastructural analysis of corticostriatal synapses in the dorsolateral striatum of aged xCT^{+/+} and xCT^{-/-} mice. A-E Neither terminal (A,B) or spine size (C,D), nor the size of the mitochondria (E) at corticostriatal synapses are different between aged xCT^{-/-} mice. F Synaptic cleft width is decreased in aged xCT^{-/-} mice, compared to the xCT^{-/-} mice (one xCT^{-/-} outlier excluded). G-I The area, thickness and length of the post-synaptic density (PSD) are unaffected by xCT deletion. J-L The glutamate (Glu) density in the pre- (J) and post-synapse (K), and in mitochondria (L) also did not differ between genotypes. Two photomicrographs are depicted representing an example of a VGLUT1-labelled corticostriatal synapse. The black arrows point towards the PSD (the red dash notes the width of the synaptic cleft, the parentheses at the synaptic cleft note the length of the PSD), while the white arrowheads indicate the gold-labelled glutamate particles. LT: labelled terminal, SP: spine. n = 6 mice for both genotypes and 25 ± 3 pictures/mouse were analyzed, with a total of 154 synapses for xCT^{-/-+} and 149 for xCT^{-/--} mice. Data are presented as mean \pm SEM and analyzed using an unpaired two-tailed t-test (A-E,G,H,J-L) or unpaired Welch's t-test (F,I): *p < 0.05; **p < 0.01.

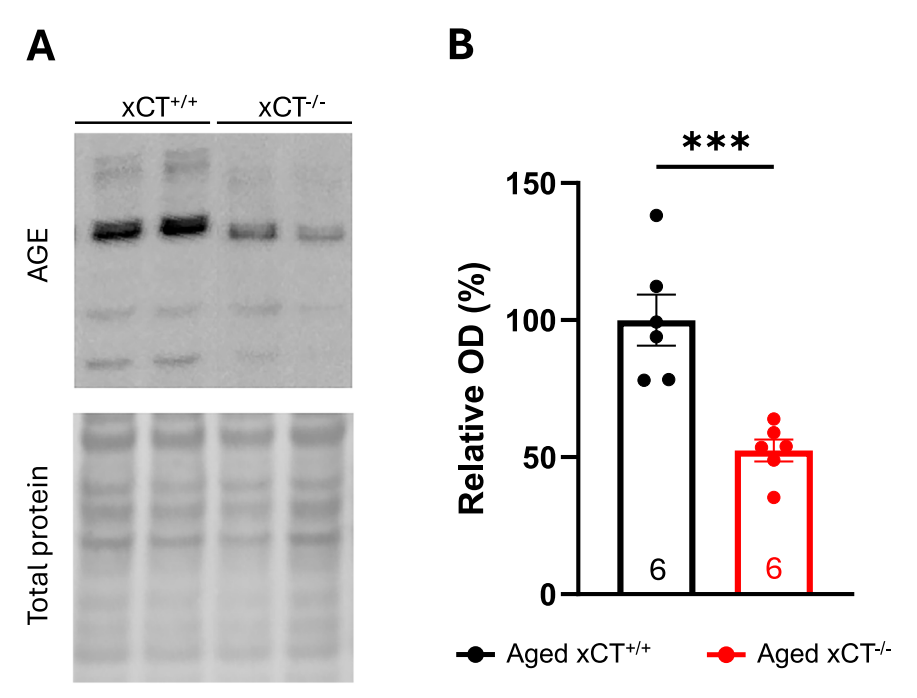


Fig. 3 Striatal AGE levels are reduced in aged xCT^{-/-} mice compared to age-matched xCT^{+/+} controls. A Representative example of AGE-positive protein bands with the according total protein stain. B Relative optical density (OD) of the immunoreactive bands, normalized to the total protein stain. Data are presented as mean \pm SEM. Analysis was performed using an unpaired two-tailed t-test. n = 6 mice/group. ***p < 0.001.

electrophysiology) or technical differences (size of the gold particles used to measure glutamate), behavioral analyses as well as Golgi Cox stainings were performed simultaneously for both age groups. Overall, both the morphology of the MSN (Suppl. Figure 2) and the ultrastructural analyses of corticostriatal synapses (Suppl. Figure 3) show age-related changes, with limited impact of xCT deletion on most of the parameters. While aging reduces the soma diameter (Suppl. Figure 2C) and the length of the longest dendrite (Suppl. Figure 2F) and increases the number of spines (Suppl. Figure 2G), it has no effect on the complexity of the dendritic tree (Suppl. Figure 2H). Aging also reduces the area (Suppl. Figure 3A) and increases the diameter of the cortical terminals (Suppl. Figure 3B), while both the area and diameter of the spines are increased (Suppl. Figure 3C, D). Interestingly, the width of the synaptic cleft is increased in adult xCT^{-/-} versus xCT^{+/+}, while aging only induces a decrease in xCT^{-/-} mice (Suppl. Figure 3E) [4, 8].

While adult xCT^{-/-} mice bury more marbles (Suppl. Figure 4A) and spend more time digging (Suppl. Figure 4B) than their agematched wildtype controls, the number of marbles they bury and the time they dig significantly decreases with aging, to reach the same value as the aged wildtype mice (Suppl. Figure 4A,B). The latency before the mice start digging in the marble burying test (Suppl. Figure 4C), is overall increased in aged mice, an effect that is mainly driven by the xCT^{+/+} mice. Only age-related effects were observed for the grooming behavior, with an overall decrease in

latency to start grooming (Suppl. Figure 4G) and the number of grooming bouts (Suppl. Figure 4H), whereas the grooming time (Suppl. Figure 4I) was increased with aging.

In the reciprocal interaction test, the total time spent in reciprocal interaction is overall decreased both with aging and by the genetic deletion of xCT, while the age-related decrease was most pronounced in the xCT^{+/+} mice (Suppl. Figure 5A). Moreover, we observe overall genotype effects in the two behaviors that can be linked to aggressive and/or dominant behavior -i.e. mounting (Suppl. Figure 5B) and crawling (Suppl. Figure 5C)- with a strong decrease in this behavior when xCT is absent. When evaluating the more exploratory behavior (Suppl. Figure 5D,E,F), it is clear that these kind of interactions are reduced in adult mice lacking xCT while showing a stronger age-related decrease in the xCT^{+/+} and not in xCT^{-/-} mice, leading to a levelling out of the differences that were initially observed in young-adult mice.

To compare data of adult and aged mice during the social interest phase of the three-chamber test, preference indexes were calculated to rule out any bias induces by reduced mobility of the aged vs. adult mice. Aged xCT^{/-} mice had an increased preference to interact with the socially naive mouse (time spent interacting with the mouse/total time interacting with mouse and object) compared to young-adult xCT^{/-} mice (Suppl. Figure 5G). The aged mice displayed a similar percentage of interaction with the socially naive mouse compared to the adult xCT^{+/+} mice, indicating the

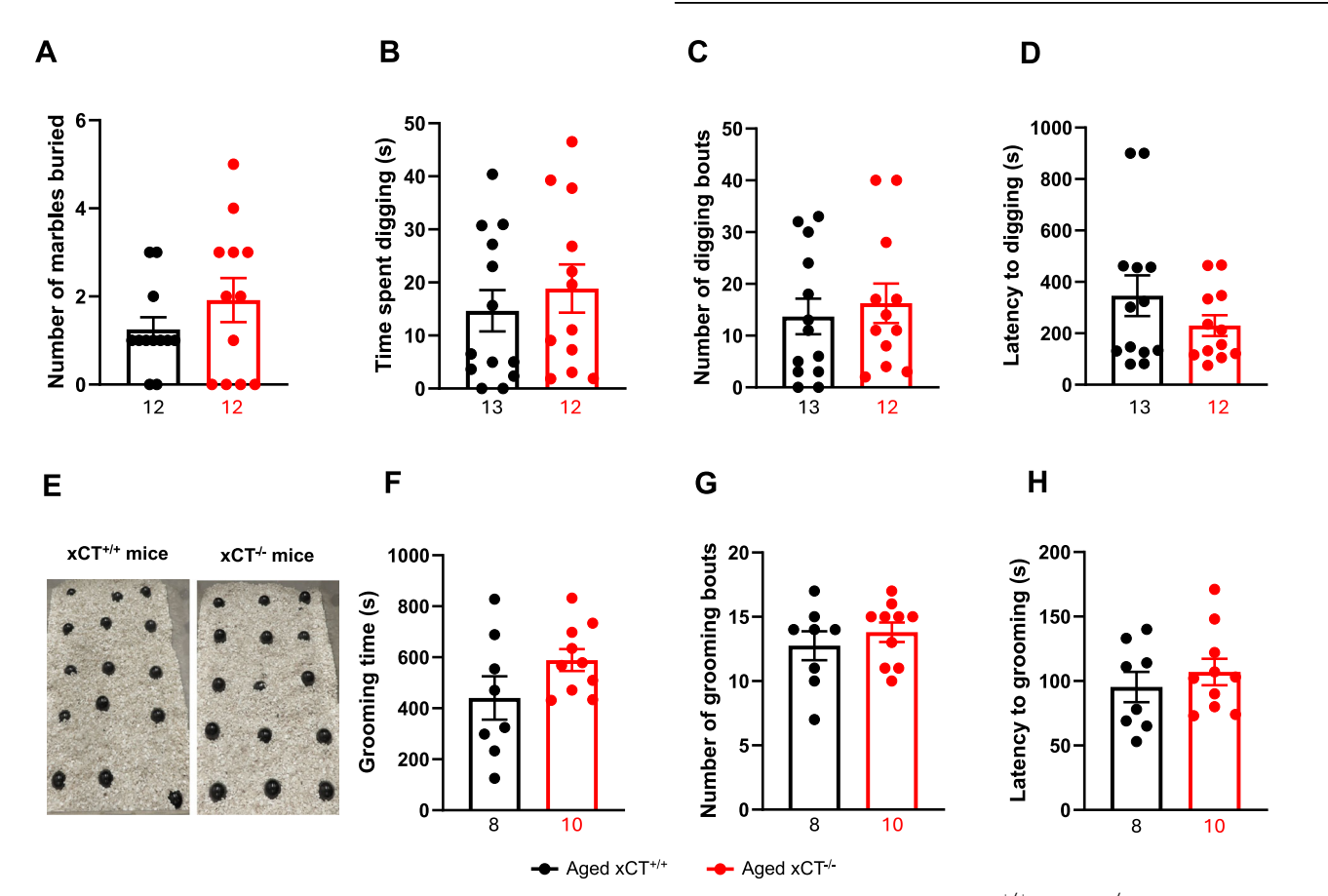


Fig. 4 No changes in repetitive behavior in aged mice lacking xCT. A–D No differences between aged xCT^{+/+} and xCT^{-/-} mice for the number of marbles buried (**A**, one xCT^{+/+} outlier excluded), time spent digging (**B**), number of digging bouts (**C**) and their latency to start digging (**D**; n = 13 xCT^{+/+} and n = 12 xCT^{-/-} mice). **E** Representative picture of a home cage with 15 black marbles after the test trial of 15 min. **F–H** The total grooming time (**F**), number of grooming bouts (**G**) and latency to start grooming (**H**) are not different between genotypes; n = 8 xCT^{+/+} mice and n = 10 xCT^{-/-} mice. Data are presented as mean \pm SEM and analyzed using a unpaired two-tailed t-test (**A–C, F–H**) or a two-tailed Mann-Whitney test (**D**).

absence of loss of interest due to aging (Suppl. Figure 5G). The preference index for entering the chamber with the mouse (time spent in chamber with mouse/total time spent in both chambers) showed that adult xCT^{-/-} mice and aged xCT^{+/+} mice spent proportionally less time in the chamber containing the mouse, compared to adult xCT^{+/+} mice (Suppl. Figure 5H). The relative number of entries in the chamber did not differ between age or genotype (Suppl. Figure 5I).

DISCUSSION

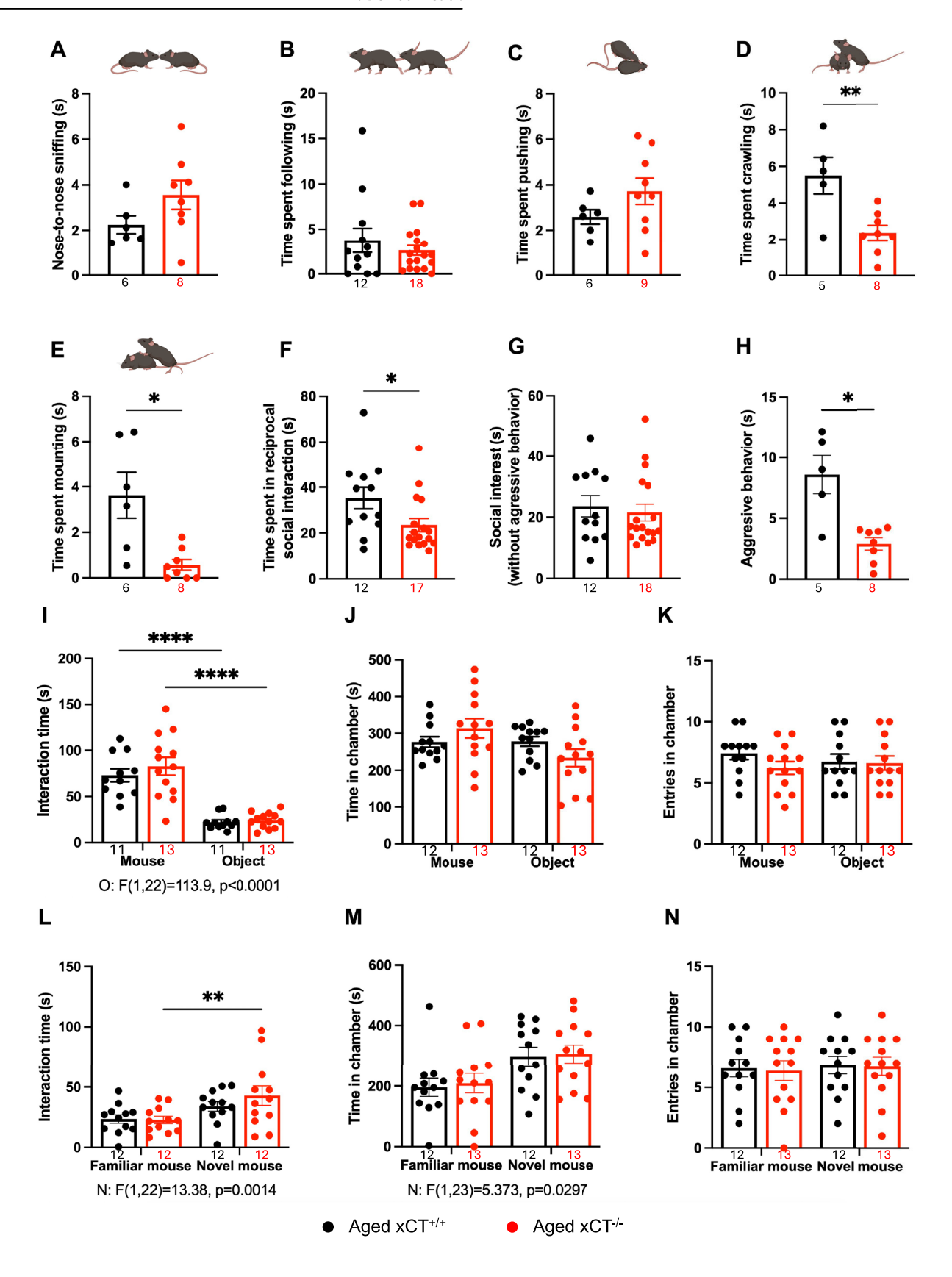
We previously reported on the presence of deficits in cortico-striatal neurotransmission that were accompanied by ASD-like behavior, in young-adult xCT^{/-} mice [8]. In the current study, we evaluated multiple parameters related to corticostriatal neurotransmission in aged xCT^{+/+} and xCT^{-/-} mice, to establish whether the previously reported deficits are persistent throughout life.

We here show that aged xCT^{/-} mice no longer present impaired corticostriatal neurotransmission or decreased intracellular glutamate levels, compared to age-matched xCT^{+/+} controls. Also, morphological differences are absent in Golgi-Cox analysis of MSNs, while ultrastructural analyses of corticostriatal synapses only revealed differences in synaptic cleft width. Furthermore, while both the reciprocal interaction test and the three-chambered test showed intact social interest in aged xCT^{/-} mice, compared to their wildtype littermates, reduced aggressive/dominant behavior was observed in the aged xCT^{/-} mice, compared to xCT^{+/+} mice, similar as in young-adult mice.

While in aged cats and rats, MSNs need higher stimulation intensities to efficiently induce action potentials -reflecting an age-related decrease in strength of corticostriatal inputs [41]- in mice it has been shown that basal corticostriatal neurotransmission is unaffected by aging [42]. Yet, the changes in corticostriatal synaptic plasticity that are reported in mice, might result from changes in receptor-activated signalling cascades linked to neuroinflammation and a more oxidative environment [42]. Given the change in electrophysiology set-up between the measurements we performed on slices of young-adult and aged mice, we cannot make any statement on age-related effects as we cannot compare the absolute values of our results in the aged mice with the results we previously reported in young-adult mice. However, whereas xCT deletion resulted in corticostriatal deficits in adult mice, this was not the case in aged mice.

We previously showed that the impaired neurotransmission in young-adult xCT^{-/-} mice, could be restored by adding exogenous glutamate to the slice, probably compensating for the reduced intracellular glutamate levels in the pre- and post-synaptic compartment of their corticostriatal synapses [8]. xCT deletion did, however, not result in reduced intracellular glutamate levels in aged mice, possibly explaining why we did not observe deficits in corticostriatal neurotransmission in aged xCT^{-/-} mice. Moreover, according to our findings in the hippocampus [4], we observed reduced AGE levels in the striatum of aged xCT^{-/-} mice, compared to xCT^{+/+} controls. AGE production and RAGE expression undergo an age-related upregulation in the brain [43] and might have a detrimental effect on the corticostriatal pathway and related





behavioral deficits [44]. Indeed, an accumulation of AGEs has been found in the brain of ASD patients [30]. The decrease in striatal AGE levels in aged xCT^{-/-} mice, might thus partly explain the absence of corticostriatal deficits. Finally, the reduced inflammatory profile that

we previously observed in aged xCT^{/-} mice [4] could also add to the anticipated beneficial effects of xCT deletion in the aged brain.

Typical age-related morphological changes in MSNs have been described -such as e.g. a decrease in the number [45] and/or

Fig. 5 xCT deletion in mice reduces dominance/aggression without affecting social interest. A-F Nose-to-nose sniffing (A, one xCT $^{-/-}$ outlier excluded), following (B) and pushing (C) are not affected by genotype, while more aggressive behaviors such as crawling (D, one xCT $^{+/+}$ and one xCT $^{-/-}$ outlier excluded) and mounting (E, one xCT $^{-/-}$ outlier excluded) are decreased in xCT $^{-/-}$ mice, compared to xCT $^{+/+}$ mice (n = 6 xCT $^{+/+}$ couples and n = 9 xCT $^{-/-}$ couples). This results in a decreased total reciprocal interaction time in xCT $^{-/-}$ mice, compared to xCT $^{+/+}$ mice (F, one xCT $^{-/-}$ outlier excluded). G, H Social interest (nose-to-nose, following, pushing) is similar between both genotypes (G), while aggressive behavior (crawling and mounting) is less pronounced in aged xCT $^{-/-}$ compared to aged xCT $^{+/+}$ mice (H, one xCT $^{+/+}$ and one xCT $^{-/-}$ outlier excluded). I In the three-chamber assay (n = 12 xCT $^{+/+}$ and n = 13 aged xCT $^{-/-}$ mice), both xCT $^{+/+}$ and xCT $^{-/-}$ mice prefer interacting with the mouse compared to the object (one xCT $^{+/+}$ outlier excluded). J, K No differences in the time spent and number of entries into the chamber with the mouse or object. L Both xCT $^{+/+}$ and xCT $^{-/-}$ mice prefer interacting with the novel mouse compared to the familiar mouse. M, N No differences in time spent (L) and number of entries (M) into the chamber with the novel or familiar mouse. Data are presented as mean ± SEM and analyzed using a two-tailed Mann-Whitney test (B, F), two-tailed unpaired t-test (A, C, D), an unpaired Welch's t-test (E, H) or a repeated-measures two-way ANOVA followed by a Sidak's post-hoc test (I-N). O: object effect, N: novel mouse effect. *p < 0.05, **p < 0.01, *******p < 0.0001.

length [46] of neuronal dendrites- whereas the effect on spine density is dependent on the type of spine [46]. We here show that most of the changes that were induced in MSNs by the aging process, were unaffected by the loss of xCT. Also, ultrastructural changes at the level of the synapse might underlie differences in corticostriatal neurotransmission. The age-related increase in terminal diameter as well as spine area and diameter, is independent of xCT and might correspond to the increase in total synaptic area that was described in humans as being a compensatory mechanism of the aged CNS to ensure sufficient transmission and release probability of neurotransmitters [47]. When synaptic size exceeds a certain limit, the synaptic contact (i.e. the PSD) can split into several pieces, thereby modifying the neuronal connectivity [47]. Yet, no difference in number of synapses associated with a perforated PSD could be detected between aged xCT^{+/+} and xCT^{-/-} mice (data not shown). Interestingly, ultrastructural analysis showed a decrease in the width of the synaptic cleft of aged xCT^{-/-} mice compared to agematched wildtype controls [10], as a result of an age-related decrease in xCT^{-/-}, but not xCT^{+/+} mice. While the optimal cleft width could vary between synapses based upon synaptic architecture, the width of the synaptic cleft will not only affect the effective concentration of neurotransmitter that is being released but can also alter the synaptic current [48]. As such, the age-related decrease that is observed in xCT^{-/-} mice might be a compensatory mechanism to restore proper synaptic neurotransmission in the aged mice. Also, the length of the PSD is reduced in aged xCT^{/-} mice compared to xCT^{+/+} mice, and genotype seems to interact with the age-related changes in PSD length, that could possibly alter the number of associated glutamate receptors.

Bentea et al. showed decreased social interaction in adult xCT^{/-} mice, compared to their wildtype littermates, as evidenced by reduced nose-to-nose sniffing, following, mounting, crawling and pushing [8]. Our study shows that aging induces an overall decrease in interaction time, while aged xCT/- mice remain less prone to social interaction compared to the aged $xCT^{+/+}$ mice. Yet, the general decrease in social interaction is solely based on decreased crawling and mounting behavior, while the more exploratory behavior is unaffected by xCT deletion. Mounting behavior between male mice is seen as aggressive, threatening behavior to assert dominance, since they will not allow the presence of unfamiliar males within their home cage [39, 40]. Therefore, xCT^{/-} mice seem to have an overall less aggressive nature, compared to xCT^{+/+} mice. As we could not link this to differences in testosterone levels between both genotypes, further research is required to confirm (or refute) this hypothesis. Together with the absence of differences between genotypes in the three-chambered assay, we conclude that aged xCT^{-/-} mice are no longer socially impaired.

In the three-chambered assay, aging induced an overall decrease in time spent interacting with both the object and the mouse. However, when evaluating the preference index, young-adult xCT^{-/-} mice showed a decreased preference for the mouse (versus the object), whereas the aged mice of both genotypes displayed a similar preference for the mouse to what was seen in

adult xCT^{+/+} mice, indicating that although overall social interaction decreases -due to lack of motivation or movement- the social interest of these mice is not affected. Age-related effects on social interaction have been sparsely investigated in mice. Some studies indicate that age-related decline of cognitive and executive functions in humans leads to deterioration of social behavior as well [49, 50]. On the other hand, others believe that social impairment might arise before the onset of other age-related impairments [51]. Similar to our study, literature states that aged mice do still have a preference to interact with mice over objects [52]. Yet, contrary to our findings on social recognition/novelty, Shoji et al. reported that 17-months-old C57BL/6 J mice lost their preference for the novel over the familiar mouse, which might be a sign of impaired social recognition [53].

In the marble burying assay, the young-adult xCT/- mice spent an increased time digging and buried an increased number of marbles compared to all other groups. Yet, while no differences could be detected between aged xCT+/+ and xCT/- mice, the compulsive behavior of the adult xCT/- mice returns to control levels with aging. Overall locomotor activity and velocity of the mice were unaffected by genotype (data not shown), excluding a possible bias of the results. The digging behavior of mice is a measure for their general well-being as well as motor function. The reasons and motivation behind increased or excessive digging behavior is still uncertain but is often seen as anxiety-like or compulsive behavior [54]. Finally, while we observed a clear age-related increase in time spent grooming -in accordance with literature [38, 55]- no genotype-related differences were detected in the aged mice.

We previously identified system x_c as the major source of extracellular glutamate in the striatum of adult mice [3]. Moreover, adult xCT^{/-} mice appeared to have decreased glutamate concentrations in both pre- and postsynaptic compartments of the corticostriatal synapses [8]. However, total striatal glutamate levels were unaffected by xCT deletion [3], thus suggesting a build-up inside the astrocytes. The importance of the decreased neuronal glutamate concentrations in adult xCT^{/-} mice was highlighted by the fact that adding glutamate to the slice in the electrophysiological set-up, rescued corticostriatal neurotransmission in adult xCT/mice [8]. It thus seems that, while in adult mice the reduced intracellular glutamate levels resulted in hampered corticostriatal neurotransmission, the reduced extrasynaptic glutamate levels might exert protective effects in aged mice. Glutamate released into the extrasynaptic space, can activate extrasynaptic glutamate receptors to modulate synaptic transmission. Yet, while activation of synaptic NMDA receptors was shown to activate pro-survival pathways, excessive activation of extrasynaptic NMDA receptors induces excitotoxicity [56]. With aging, NMDA receptors were shown to migrate from the synaptic cleft to the extrasynaptic space [57], and the reduced extrasynaptic glutamate levels that are seen in the absence of xCT might thus be particularly protective in the aged brain or age-related neurological disorders. Memantine, an NMDA receptor antagonist that blocks preferentially extrasynaptic receptors [58], is used for the treatment of Alzheimer's disease patients. Although controversial, memantine has been shown to be a safe

Table 1. Overview of the	Overview of the effect of xCT deletion in adult and aged mice.	adult and aged mice.				
EXPERIMENT		t-test/Mann-Whitney		Two-way ANOVA		
		Adult xCT ^{-/-} vs adult xCT +/+	Aged xCT ^{-/-} vs aged xCT ^{+/+}	Age effect (both genotypes aged vs. adult)	Genotype effect (both age groups xCT ^{-/-} vs. xCT ^{-/-})	AgexGenotype INTERACTION
Corticostriatal slice	- I/O curve	>	ns			
electrophysiology	- paired pulse ratio	ns	ns			
Golgi-Cox analysis	- Soma diameter	ns	ns	✓ p<0.05 no significant post-hoc	ns	ns
	- Length of longest dendrite	ns	ns	✓ p<0.05 no significant post-hoc	ns	ns
	- Spine density	ns	ns	\sim p<0.01 xCT ^{+/+} aged > adult p=0.02224 xCT ^{-/-} aged vs adult: ns	ns	ns
Ultrastructural analysis	- Terminal area	ns	ns	\sim p<0.001 xCT+/+aged vs adult: ns xCT- $^{\prime}$ aged < adult, p=0.0014	ns	ns
	- Terminal diameter	ns	ns	\sim p<0.001 xCT ^{+/+} aged > adult, p=0.0031 xCT ^{-/-} aged vs adult: ns	ns	ns
	- Spine area	ns	ns	\sim p<0.001 xCT ^{+/+} aged > adult, p=0.0025 xCT ^{-/-} aged > adult, p=0.0144	ns	ns
	- Spine diameter	ns	ns	\sim p<0.0001 xCT ^{+/+} aged > adult, p=0.0003 xCT ^{-/-} aged > adult, p=0.0003	ns	ns
	- Synaptic cleft width	ns	>	NA	NA	p < 0.01 $adult xCT^{+/+} < xCT^{-},$ p = 0.0230 $xCT^{-/} adult > aged,$ p = 0.0016
	- Mitochondrial area	ns	ns	\sim p<0.0001 xCT ^{+/+} aged < adult, p=0.0009 xCT ^{-/-} aged < adult, p<0.0001	ns	ns
	- PSD length	ns	>	NA	NA	p<0.05 no significant post-hoc
	- Glutamate levels	>	ns			
Marble burying	- marbles buried	<	ns	NA	NA	p < 0.05 $adult xCT^{+/+} < xCT^{-'}$, p = 0.0017 $xCT^{-'}adult > aged$, p = 0.0014
	- time spent digging	<	ns	NA	NA	p<0.01 adult xCT +/+< xCT', p<0.0001 xCT-*adult > aged, p<0.0001
	- latency to digging	ns	ns	\sim p<0.01 xCT ^{+/+} aged > adult, p=0.0154 xCT ^{-/-} aged vs adult: ns	ns	ns
	- digging bouts	<	ns	\sim p<0.001 xCT+/+aged vs adult: ns xCT-' aged < adult, p=0.0018	ns	ns

Table 1. continued						
EXPERIMENT		t-test/Mann-Whitney		Two-way ANOVA		
		Adult xCT ^{-/-} vs adult xCT +/+	Aged xCT ^{-/-} vs aged xCT ^{+/+}	Age effect (both genotypes aged vs. adult)	Genotype effect (both age groups $xCT^{-\ell}$ vs. $xCT^{+\ell+1}$)	AgexGenotype INTERACTION
Grooming behaviour	- latency to groom	ns	ns	✓ p<0.01 no significant post-hoc	ns	ns
	- number of grooming bouts	SU	ns	\sim p<0.01 xCT ^{+/+} aged < adult, p=0.0031 xCT ^{-/-} aged vs adult: ns	ns	ns
	- grooming time	SU	ns	\sim p<0.0001 xCT ^{+/+} aged > adult, p=0.0051 xCT ^{-/-} aged > adult, p<0.0001	ns	ns
Reciprocal social interaction	- total time	>	>	\sim p<0.001 xCT+'+aged < adult, p=0.0138 xCT-'- aged vs adult: ns	$\sim p < 0.01$ $adult \ xCT^{+/-} \times xCT^{+/+} \ p = 0.0233$ $aged \ xCT^{+} \lor v \ xCT^{+/+} : ns$	ns
	- nose-to-nose	>	ns	NA	NA	p < 0.01 $xCT^{+/+}adult > aged,$ p = 0.0006 $adult xCT^{+/+} > xCT^{-/-},$ p = 0.0132
	- following	>	ns	\sim p<0.0001 xCT ^{+/+} aged < adult, p=0.0001 xCT ^{-/-} aged < adult, p=0.0244	\sim p<0.05 adult xCT $^{+}$ < xCT $^{++}$ p=0.0484 aged xCT $^{+}$ vs xCT $^{++}$ +. ns	ns
	- mounting	>	>	ns	> p<0.0001 adult xCT ^{-/-} < xCT ^{+/+} , p=0.0036 aged xCT ^{-/-} < xCT ^{+/+} , p=0.0019	ns
	- crawling	>	>	ns	\sim p<0.01 adult xCT $^{-4}$ vs xCT $^{+/4}$: ns aged xCT $^{-4}$ < xCT $^{+/4}$, p=0.0303	ns
	- pushing	>	ns	\sim p<0.001 xCT+'+aged < adult, p=0.0011 xCT-'- aged vs adult: ns	ns	ns
Three-chambered assay: social preference	- interaction with mouse	>	ns	NA	NA	p < 0.01 $xCT^{+/+}adult > aged,$ p < 0.0001 $adult xCT^{+/+} > xCT^{-/-},$ p = 0.0063
	- time in chamber: mouse	ns	ns	NA	NA	p<0.05 no significant post-hoc
	- entries in chamber: mouse	ns	ns	\sim p<0.0001 xCT ^{+/+} aged < adult, p=0.0014 xCT ^{-/} aged < adult, p=0.0011	ns	ns

results sections, this comparison is done by a t-test or Mann-Whitney test. A and V indicate an increase or a decrease, respectively. In the third column, we combined data of both studies and used a two-way ANOVA followed by a multiple comparison analysis (post-hoc test), to identify age- and genotype effects. Slice electrophysiology data and glutamate analysis were not compared using a two-way ANOVA due to technical issues. A and V indicate the sense of the main effects of the two-way ANOVA, while the results of the post-hoc are indicated just below. See Supplementary figures for the corresponding graphs. (ns = not significant, NA = not applicable) In this table, the second column summarizes the data obtained in adult (Bentea et al., 2021) as well as aged mice (current study), and compares genotypes within one age group. As described in the respective

and effective intervention for neuropsychiatric disorders, including OCD and ASD [59].

To conclude, contrary to what we observed in adult xCT^{-/-} mice, the deletion of xCT did not result in corticostriatal dysfunction or altered social or repetitive behavior in aged mice. Whether these age-related differences are related to a restoration of corticostriatal neurotransmission during the aging process in xCT^{-/-} mice or an age-related decrease in corticostriatal transmission in xCT^{+/+} and not xCT^{-/-} mice, remains elusive and requires additional experiments. Yet, the absence of corticostriatal impairment in aged xCT^{-/-} versus xCT^{+/+} mice, is an important finding on its own as targeting xCT has been proposed as a potential strategy in the treatment of age-related neurological disorders [3, 11].

DATA AVAILABILITY

The data that support the findings of this study are available upon reasonable request (to the corresponding author AM).

REFERENCES

- Lewerenz J, Hewett SJ, Huang Y, Lambros M, Gout PW, Kalivas PW, et al. The cystine/ glutamate antiporter system xc- in health and disease: from molecular mechanisms to novel therapeutic opportunities. Antioxid Redox Signal. 2013;18:522–55.
- 2. De Bundel D, Schallier AS, Loyens E, Fernando R, Miyashita H, van Liefferinge J, et al. Loss of system x(c)- does not induce oxidative stress but decreases extracellular glutamate in hippocampus and influences spatial working memory and limbic seizure susceptibility. J Neurosci. 2011;31:5792–803.
- Massie A, Schallier A, Kim SW, Fernando R, Kobayashi S, Beck H, et al. Dopaminergic neurons of system xc-deficient mice are highly protected against 6hydroxydopamine-induced toxicity. FASEB J. 2011;25:1359–69.
- Verbruggen L, Ates G, Lara O, De Munck J, Villers A, De Pauw L, et al. Lifespan extension with preservation of hippocampal function in aged system xc—deficient male mice. Mol Psychiatry. 2022;27:2355–68.
- Massie A, Boillée S, Hewett S, Knackstedt L, Lewerenz J. Main path and byways: non-vesicular glutamate release by system x_c⁻ as an important modifier of glutamatergic neurotransmission. J Neurochem. 2015;135:1062–79.
- Domercq M, Sánchez-Gómez MV, Sherwin C, Etxebarria E, Fern R, Matute C. System xc— and glutamate transporter inhibition mediates microglial toxicity to oligodendrocytes. Journal Immunol. 2007;178:6549–56.
- Kigerl KA, Ankeny DP, Garg SK, Wei P, Guan Z, Lai W, et al. System xc regulates microglia and macrophage glutamate excitotoxicity in vivo. Exp Neurol. 2012;233:333–41.
- Bentea E, Villers A, Moore C, Funk AJ, O'Donovan SM, Verbruggen L, et al. Corticostriatal dysfunction and social interaction deficits in mice lacking the cystine/glutamate antiporter. Mol Psychiatry. 2021;26:4754–69.
- Baker DA, Xi ZX, Shen H, Swanson CJ, Kalivas PW. The origin and neuronal function of in vivo nonsynaptic glutamate. J Neurosci. 2002;22:9134–41.
- Leclercq K, Van Liefferinge J, Albertini G, Neveux M, Dardenne S, Mairet-Coello G, et al. Anticonvulsant and antiepileptogenic effects of system xc

 inactivation in chronic epilepsy models. Epilepsia. 2019;60:1412

 23.
- Bentea E, De Pauw L, Verbruggen L, Winfrey LC, Deneyer L, Moore C, et al. Aged xCT-deficient mice are less susceptible for lactacystin-, but Not 1-methyl-4-phenyl-1,2,3,6- tetrahydropyridine-, induced degeneration of the nigrostriatal pathway. Front Cell Neurosci. 2021;15:796635
- Mesci P, Zaïdi S, Lobsiger CS, Millecamps S, Escartin C, Seilhean D, et al. System xC

 is a mediator of microglial function and its deletion slows symptoms in amyotrophic lateral sclerosis mice. Brain. 2015;138:53–68.
- Bentea E, Demuyser T, Van Liefferinge J, Albertini G, Deneyer L, Nys J, et al. Absence of system xc- in mice decreases anxiety and depressive-like behavior without affecting sensorimotor function or spatial vision. Prog Neuropsychopharmacol Biol Psychiatry. 2015;59:49–58.
- Albertini G, Deneyer L, Ottestad-Hansen S, Zhou Y, Ates G, Walrave L, et al. Genetic deletion of xCT attenuates peripheral and central inflammation and mitigates LPS-induced sickness and depressive-like behavior in mice. Glia. 2018;66:1845–61.
- Lewerenz J, Baxter P, Kassubek R, Albrecht P, Van Liefferinge J, Westhoff M-A, et al. Phosphoinositide 3-kinases upregulate system xc(-) via eukaryotic initiation factor 2α and activating transcription factor 4 - A pathway active in glioblastomas and epilepsy. Antioxid Redox Signal. 2014;20:2907–22.
- Ashraf A, Jeandriens J, Parkes HG, So P-W. Iron dyshomeostasis, lipid peroxidation and perturbed expression of cystine/glutamate antiporter in alzheimer's disease: Evidence of ferroptosis. Redox Biol. 2020;32:101494.

- Kazama M, Kato Y, Kakita A, Noguchi N, Urano Y, Masui K, et al. Astrocytes release glutamate via cystine/glutamate antiporter upregulated in response to increased oxidative stress related to sporadic amyotrophic lateral sclerosis. Neuropathology. 2020;40:587–98.
- Pampliega O, Domercq M, Soria FN, Villoslada P, Rodríguez-Antigüedad A, Matute C. Increased expression of cystine/glutamate antiporter in multiple sclerosis. J Neuroinflammation. 2011;8:63–75.
- Merckx E, Albertini G, Paterka M, Jensen C, Albrecht P, Dietrich M, et al. Absence of system xc — on immune cells invading the central nervous system alleviates experimental autoimmune encephalitis. J Neuroinflammation. 2017;14:9.
- Robert SM, Buckingham SC, Campbell SL, Robel S, Holt KT, Ogunrinu-Babarinde T, et al. SLC7A11 expression is associated with seizures and predicts poor survival in patients with malignant glioma. Sci Transl Med. 2015;7:289ra86.
- Jung WH, Kang DH, Kim E, Shin KS, Jang JH, Kwon JS. Abnormal corticostriatallimbic functional connectivity in obsessive-compulsive disorder during reward processing and resting-state. Neuroimage Clin. 2013;3:27–38.
- Welch JM, Lu J, Rodriguiz RM, Trotta NC, Peca J, Ding JD, et al. Cortico-striatal synaptic defects and OCD-like behaviours in Sapap3-mutant mice. Nature. 2007;448:894–900.
- Li W, Pozzo-Miller L. Dysfunction of the corticostriatal pathway in autism spectrum disorders. J Neurosci Res. 2020;98:2130–47.
- Jia YF, Wininger K, Peyton L, Ho AMC, Choi DS. Astrocytic glutamate transporter 1 (GLT1) deficient mice exhibit repetitive behaviors. Behav Brain Res. 2021;396:112906.
- 25. Liu Y, Sun Y, Chen A, Chen J, Zhu T, Wang S, et al. Involvement of disulfidptosis in the pathophysiology of autism spectrum disorder. Life Sci. 2025;369:123531.
- Dickinson A, Jeste S, Milne E. Electrophysiological signatures of brain aging in autism spectrum disorder. Cortex. 2022;148:139–51.
- Hand BN, Angell AM, Harris L, Carpenter LA. Prevalence of physical and mental health conditions in medicare-enrolled, autistic older adults. Autism. 2020;24:755–64.
- 28. Zhang Y, Zhang Z, Tu C, Chen X, He R. Advanced glycation end products in disease development and potential interventions. Antioxidants. 2025;14:492.
- Anwar A, Abruzzo PM, Pasha S, Rajpoot K, Bolotta A, Ghezzo A, et al. Advanced glycation endproducts, dityrosine and arginine transporter dysfunction in autism - a source of biomarkers for clinical diagnosis. Mol Autism. 2018:9:3.
- Junaid MA, Kowal D, Barua M, Pullarkat PS, Sklower Brooks S, Pullarkat RK. Proteomic studies identified a single nucleotide polymorphism in glyoxalase I as autism susceptibility factor. Am J Med Genet A. 2004;131A:11–7.
- Sato H, Shiiya A, Kimata M, Maebara K, Tamba M, Sakakura Y, et al. Redox imbalance in cystine/glutamate transporter-deficient mice. J Biol Chem. 2005;280:37423–9.
- Villers A, Ris L. Improved preparation and preservation of hippocampal mouse slices for a very stable and reproducible recording of long-term potentiation. J Vis Exp. 2013:26:50483.
- Aerts J, Nys J, Moons L, Hu TT, Arckens L. Altered neuronal architecture and plasticity in the visual cortex of adult MMP-3-deficient mice. Brain Struct Funct. 2015;220:2675–89.
- 34. Toy WA, Petzinger GM, Leyshon BJ, Akopian GK, Walsh JP, Hoffman MV, et al. Treadmill exercise reverses dendritic spine loss in direct and indirect striatal medium spiny neurons in the 1-methyl-4-phenyl-1,2,3,6-tetrahydropyridine (MPTP) mouse model of Parkinson's disease. Neurobiol Dis. 2013;63:201–9.
- Bentea E, Sconce MD, Churchill MJ, Van Liefferinge J, Sato H, Meshul CK, et al. MPTP-induced parkinsonism in mice alters striatal and nigral xCT expression but is unaffected by the genetic loss of xCT. Neurosci Lett. 2015;593:1–6.
- 36. Chang YC, Cole TB, Costa LG. Behavioral phenotyping for autism spectrum disorders in mice. Curr Protoc Toxicol. 2017;72:1–21.
- 37. Deacon RMJ. Digging and marble burying in mice: simple methods for in vivo identification of biological impacts. Nat Protoc. 2006;1:122–4.
- Kalueff AV, Wayne Aldridge J, Laporte JL, Murphy DL, Tuohimaa P. Analyzing grooming microstructure in neurobehavioral experiments. Nat Protoc. 2007;2:2538–44.
- Theil JH, Ahloy-Dallaire J, Weber EM, Gaskill BN, Pritchett-Corning KR, Felt SA, et al. The epidemiology of fighting in group-housed laboratory mice. Sci Rep. 2020;10:16649.
- 40. Zoicas I, Kornhuber J. The role of metabotropic glutamate receptors in social behavior in rodents. Int J Mol Sci. 2019;20:1412.
- Walsh JP, Akopian G. Physiological aging at striatal synapses. J Neurosci Res. 2019:97:1720–7.
- Chepkova AN, Schönfeld S, Sergeeva OA. Age-related alterations in the expression of genes and synaptic plasticity associated with nitric oxide signaling in the mouse dorsal striatum. Neural Plast. 2015;2015:458123.
- Semchyshyn H. Is carbonyl/AGE/RAGE stress a hallmark of the brain aging?. Pflugers Arch. 2021;473:723–34.
- 44. Maher P. Methylglyoxal, advanced glycation end products and autism: is there a connection?. Med Hypotheses. 2012;78:548–52.

- Rafols JA, Cheng HW, McNeill TH. Golgi study of the mouse striatum: age-related dendritic changes in different neuronal populations. J Comp Neurol. 1989:279:212–27.
- 46. Dickstein DL, Weaver CM, Luebke JI, Hof PR. Dendritic spine changes associated with normal aging. Neuroscience. 2013;251:21–32.
- Bertoni-Freddari C, Fattoretti P, Pieroni M, Meier-Ruge W, Ulrich J. Enlargement of synaptic size as a compensative reaction in aging and dementia. Pathol Res Pr. 1992;188:612–5.
- 48. Savtchenko LP, Rusakov DA. The optimal height of the synaptic cleft. Proc Natl Acad Sci USA. 2007;104:1823–8.
- Bottiroli S, Cavallini E, Ceccato I, Vecchi T, Lecce S. Theory of mind in aging: comparing cognitive and affective components in the faux pas test. Arch Gerontol Geriatr. 2016;62:152–62.
- Johansson Nolaker E, Murray K, Happé F, Charlton RA. Cognitive and affective associations with an ecologically valid test of theory of mind across the lifespan. Neuropsychology. 2018;32:754–63.
- 51. Boyer F, Jaouen F, Ibrahim EC, Gascon E. Deficits in social behavior precede cognitive decline in middle-aged mice. Front Behav Neurosci. 2019;13:55.
- Greene SM, Klein PR, Alcala G-A, Bustamante I, Bordas B, Johnson A, et al. Aging to 24 months increased C57BL/6J mouse social sniffing and hippocampal Neto1 levels, and impaired female spatial learning. Behav Process. 2023;211:104929.
- Shoji H, Miyakawa T. Age-related behavioral changes from young to old age in male mice of a C57BL/6J strain maintained under a genetic stability program. Neuropsychopharmacol Rep. 2019;39:100–18.
- Pond HL, Heller AT, Gural BM, McKissick OP, Wilkinson MK, Manzini MC. Digging behavior discrimination test to probe burrowing and exploratory digging in male and female mice. J Neurosci Res. 2021;99:2046–58.
- Kalueff AV, Stewart AM, Song C, Berridge KC, Graybiel AM, Fentress JC. Neurobiology of rodent self-grooming and its value for translational neuroscience. Nat Rev Neurosci. 2016;17:45–59.
- Dong XX, Wang Y, Qin ZH. Molecular mechanisms of excitotoxicity and their relevance to pathogenesis of neurodegenerative diseases. Acta Pharm Sin. 2009;30:379–87.
- Yu SP, Jiang MQ, Shim SS, Pourkhodadad S, Wei L. Extrasynaptic NMDA receptors in acute and chronic excitotoxicity: implications for preventive treatments of ischemic stroke and late-onset Alzheimer's disease. Mol Neurodegener. 2023;18:43.
- Xia P, Chen H, Sheng V, Zhang D, Lipton SA. Memantine preferentially blocks extrasynaptic over synaptic NMDA receptor currents in hippocampal autapses. J Neurosci. 2010;30:11246–50.
- Lu S, Nasrallah HA. The use of memantine in neuropsychiatric disorders: an overview. Ann Clin Psychiatry. 2018;30:234–48.

ACKNOWLEDGEMENTS

This work was supported by a Strategic Research Program of the Vrije Universiteit Brussel (SRP85 to AM), by the Fonds de la Recherche Scientifique – FNRS under Grant No 20220719 (to LR) and by the Research Foundation Flanders - FWO under Grant No G011220N to AM, FWO-Aspirant fellowship 116580N to LPD and 11C2719N to OL, and a FWO postdoctoral fellowship 12B3223N to GA.

AUTHOR CONTRIBUTIONS

LDP, EB and AM designed the research; LDP, AV, CM, OL, OV, LV, GA and CKM contributed to the experimental execution, data collection and analysis; LA, HS, LR and AM contributed to the resources and/or provided access to research infrastructure; LDP, GA and AM prepared the manuscript draft; all authors reviewed and edited the final draft.

COMPETING INTERESTS

The authors declare no competing interests.

ETHICS APPROVAL

All animal procedures were performed according to national guidelines on animal experimentation and approved by the Ethical Committee for Animal Experimentation of the Vrije Universiteit Brussel (CEP 20-275-8; 20-275-OC1). This study did not involve human subjects.

ADDITIONAL INFORMATION

Supplementary information The online version contains supplementary material available at https://doi.org/10.1038/s41398-025-03686-9.

Correspondence and requests for materials should be addressed to Ann Massie.

Reprints and permission information is available at http://www.nature.com/reprints

Publisher's note Springer Nature remains neutral with regard to jurisdictional claims in published maps and institutional affiliations.



Open Access This article is licensed under a Creative Commons Attribution-NonCommercial-NoDerivatives 4.0 International License.

which permits any non-commercial use, sharing, distribution and reproduction in any medium or format, as long as you give appropriate credit to the original author(s) and the source, provide a link to the Creative Commons licence, and indicate if you modified the licensed material. You do not have permission under this licence to share adapted material derived from this article or parts of it. The images or other third party material in this article are included in the article's Creative Commons licence, unless indicated otherwise in a credit line to the material. If material is not included in the article's Creative Commons licence and your intended use is not permitted by statutory regulation or exceeds the permitted use, you will need to obtain permission directly from the copyright holder. To view a copy of this licence, visit http://creativecommons.org/licenses/by-nc-nd/4.0/.

© The Author(s) 2025